JOURNAL OF APPLIED ELECTROCHEMISTRY **10** (1980) 61–70

The cause of residual capacity in nickel oxyhydroxide electrodes

R. BARNARD, G. T. CRICKMORE, J. A. LEE, F. L. TYE

Berec Group Limited, Group Technical Centre, St. Ann's Road, London N15, UK

Received 6 February 1979

Chemical analysis, X-ray diffraction and linear sweep voltammetry have been used to examine the cause of the secondary discharge plateau associated with the inefficient reduction of sintered plate NiOOH electrodes. The techniques confirm the presence of β-$Ni(OH)_2$, β-NiOOH and γ-NiOOH in electrodes after failure at high rates. No evidence was obtained in support of the plateau arising from a new intrinsically less active compound. In disagreement with previous claims the γ-phase formed on overcharging was found to discharge as efficiently as the β-phase. Inefficient discharge is considered to be caused by an insulating barrier layer of β-$Ni(OH)_2$ between the charged active material and the current collector. The complex non-linear current–potential behaviour, exhibited by the secondary discharge plateau near -200 mV, is considered to be caused by the removal of Ni^{3+} or Ni^{4+} defects from the electronically conducting $Ni(OH)_2$ prior to returning it to the poorly conducting divalent state.

1. Introduction

Previous charge/discharge efficiency measurements [1] on sintered plate nickel hydroxide electrodes have drawn attention to the presence of an appreciable quantity (10–50%) of charged active material remaining after discharge at moderate to high rates. In common with other workers [2–6] it has been demonstrated that when this material is discharged at sufficiently low rates it gives rise to a second discharge plateau at least 300 mV more negative than normal.

Foerster [6] and Zedner [7, 8] considered that this low potential plateau was caused by the reduction of molecular oxygen occluded within the graphite present in their electrodes. However, Bode *et al.* [9] showed that the effect was observed in the absence of graphite and could find no evidence of intermediates symptomatic of oxygen reduction, e.g. H_2O_2. Labat [10] could similarly find no evidence in favour of oxygen adsorption from *in situ* magnetic susceptibility measurements.

Several groups of workers [2–6] have suggested that the lower potential plateau may be caused by discharge of an intrinsically less active material. Compounds such as $Ni_3O_2(OH)_4$ or $Ni_3O_4 \cdot xH_2O$ have been proposed [2, 3] as intermediates in the reduction of β-NiOOH. However, Falk [11] was unable to find any evidence of such materials. Briggs and co-workers [12, 13] concluded that the diffraction pattern for $Ni_3O_2(OH)_4$ could be equally well explained by a mixture of β-NiOOH and β-$Ni(OH)_2$. According to Tuomi [14], γ- or α-NiOOH is less active than β-NiOOH and only discharges appreciably at very low rates. Harivel *et al.* [15] have also claimed that the discharge efficiency of chemically prepared γ-NiOOH is poor. In contrast, Russian workers [16] have demonstrated that the low temperature performance of the γ-phase is superior to the β-phase and claim [17] 20–30% greater capacities for this material using high rates at normal and elevated temperatures.

The purpose of this paper is two-fold. In the first instance it provides independent data regarding the characterization of the positive active material produced in sintered plate electrodes under various charge regimes. This information will be drawn upon in further fundamental studies concerning the discharge mechanism of the nickel oxyhydroxide electrode [18]. Secondly, because of conflicting claims regarding the relationship between the low potential plateau and the form of

0021–891X/80/010061–10$03.00/0

the charged active material, it was considered important to conduct further investigations. This aspect is particularly relevant to the operation of commercial nickel–cadmium battery systems.

2. Experimental

2.1. *Electrode material and electrolyte*

The electrodes were made from nickel sinter impregnated with chemically precipitated nickel hydroxide [1]. The sample size commonly employed was 3·0 x 3·0 cm (thickness 0·065 cm) and the electrodes contained 0·81 g $Ni(OH)_2$. The nominal capacities were taken to be 234 mA h. The electrolyte (30 wt% KOH) was made from 'Pearce' technical grade flake and singly distilled water.

2.2. *Discharge capacity measurements*

The polypropylene test cells employed cylindrical nickel sheet counter electrodes and Hg/HgO reference electrodes with associated Luggin capillaries. Test electrodes were operated under 'flooded' electrolyte conditions (150 ml) at an ambient temperature 25 ± 0·5° C. A Leeds and Northrup Speedomax 'W' multi-point recorder was used to plot the galvanostatic polarization curves. A unity-gain, FET input, operational amplifier buffer was used to increase the input impedance of the recorder to $\sim 10^{12}\ \Omega$ and so minimize current drawn from the electrodes.

2.3. *Linear sweep voltammetry*

Sweep measurements were performed using a Chemical Electronics potentiostat (TR40/3A) and linear sweep unit (LSU1). Voltammograms were recorded on an *X–Y* plotter (Bryans 21004). Potentials are referred to Hg/HgO/30% KOH.

2.4. *X-ray diffraction studies*

Diffraction patterns were obtained using a Phillips X-ray diffractometer employing Ni filtered CuKα radiation (40 kV) at a scan rate of $1/2^\circ\ min^{-1}$. Samples of electrodes were removed during charge or discharge and dried as thoroughly as possible between filter papers. Additional patterns were obtained from vacuum-dried powder samples taken from sintered plate electrodes. Powder samples were packed into an aluminium cavity for X-ray examination.

In the case of the complete electrodes still in the damp state, X-ray measurements were generally made within 1 h of the sample being removed from the flooded cell. In the case of powdered samples the delay was at least 3–4 h. However, because β-NiOOH and γ-NiOOH are relatively stable no changes in X-ray diffraction behaviour could be seen even 24 h later. It is possible that α-$Ni(OH)_2$ produced by discharge of γ-NiOOH could have escaped detection because of its reversion to β-$Ni(OH)_2$. In addition phases having highly distorted layer structures which tend to be amorphous to X-rays could also have escaped detection by the procedures involved [18]. As will be discussed later the experimental results can be explained adequately on the basis of well-known nickel oxyhydroxide species found to be present.

2.5. *Available pore volume measurements*

Available pore volumes in uncycled sintered plate electrodes (3 cm x 3 cm) were evaluated from the gain in weight after vacuum impregnation with water. Surplus water was removed from the electrode surface by filter paper. With care reproducibility was found to be about ± 5%.

2.6. *Analytical techniques*

Electrodes were analysed for Ni metal and $Ni(OH)_2$ content by measurement of the volume of hydrogen evolved on dissolution of the sample in 11 M HCl followed by conventional EDTA titration with the resulting solution.

The state of charge of the electrodes (active oxygen content) was determined by a modification of the back-titration procedure of Kroger and Cattoti [19] using ferrous ammonium sulphate and potassium permanganate. The sulphuric acid concentration present during reduction of active material by Fe(II) was found to be critical in order to avoid errors from co-reduction via nickel sinter. The reduction was performed at 0° C to minimize the decomposition of Ni(III)/(IV) species. Even with the minimum acid concentration to prevent

precipitation of Fe(III) it was necessary to apply a blank correction using nickel sinter alone. Phosphoric acid added prior to titration removed by complexation the yellow colour due to Fe(III) and permitted a sharp green to pink colour change at the endpoint. It was essential to remove the 'extracted' nickel sinter before addition of the phosphoric acid to prevent further reduction of the permanganate.

Total K^+ contents of electrodes in various states of charge and discharge were determined by carefully removing surplus electrolyte with filter paper and immediately dissolving the whole electrode in 11 M HCl. The solutions were analysed for K^+ by atomic absorption spectrophotometry (Varian Techtron AA5).

3. Results and discussion

3.1. *Characterization of active material*

X-ray diffraction and 'active oxygen' measurements were combined to establish the nature of the active material produced under various charge regimes.

Fig. 1a is a diffraction pattern for a sample of unused electrode material. As expected from the method of preparation the pattern is characteristic [11–14] of β-$Ni(OH)_2 \cdot xH_2O$ having lines at 2θ angles of 19·1°, 31·1°, 38·5°, 59·1°, 62·7°, 70° and 73° (CuKα radiation). The additional lines at 44·5° and 51·7° are due to the nickel sinter.

An estimate of the $Ni(OH)_2$ crystallite size was obtained using the Scherrer equation [20]. Line broadening due to the CuK$\alpha_1\alpha_2$ doublet was neglected but a correction for instrument broadening was applied. The $D_{h,k,l}$ values implied a crystallite size in the range 20–100 nm which is of the expected order [21, 22].

Fig. 1b shows a diffraction pattern obtained from the surface of a complete electrode charged at the $C/2$ rate for 12 h. High charge rates and prolonged overcharging are claimed [14, 15, 17] to favour the formation of γ-NiOOH. Fig. 1b with new lines at $2\theta = 12{\cdot}6°$, 25·4°, 43° and 65–68° agrees well with the diffraction data reported for this phase [14, 23, 24]. Similarly a powdered sample of electrode charged under the same regime was identical to Fig. 1b with a total absence of β-phase lines. This suggests that the active material is uniformly γ-NiOOH throughout the electrode.

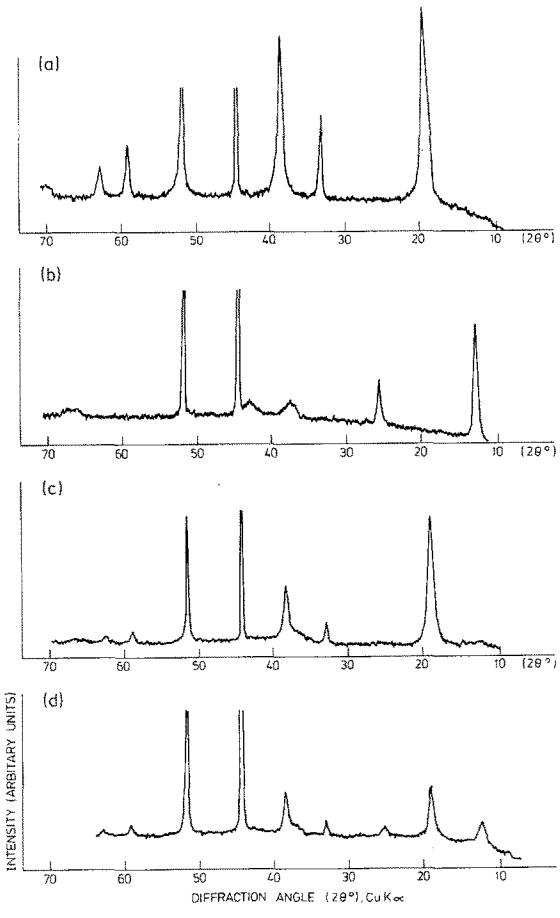

Fig. 1. X-ray diffraction patterns for: (a) Uncycled, aged, β-$Ni(OH)_2$; (b) Active material at the surface of a plate charged at the $C/2$ rate for 12 h (γ-NiOOH); (c) Active material at the surface of a plate charged at the $C/16$ rate for 24 h (β-NiOOH); (d) Powdered sample removed from a plate charged at the $C/16$ rate for 24 h (β + γ-NiOOH).

Figs. 1c and d show respectively diffraction patterns for the complete electrode surface and for a powdered sample both of which had been charged at the $C/16$ rate for 24 h. Fig. 1c contains only β-lines, the pattern resembling Fig. 1a except that the lines at $2\theta = 33°$ and 37–38° are reduced in intensity relative to the line at 19°. Consequently the active material at the surface is considered to be a mixture of β-NiOOH and β-$Ni(OH)_2$. The slight changes in intensity reflect the close similarities in crystal structure for both the oxidized and reduced species which has been well documented [11–14, 23]. On this basis the oxidation of β-$Ni(OH)_2$ is considered to occur topotactically and the diminished line intensities

are indicative of the formation of a defect layer structure. Fig. 1d indicates that γ-NiOOH is present in the electrode interior since additional lines can be seen at $2\theta = 12{\cdot}6^\circ$ and $25{\cdot}4^\circ$. Electrodes subjected to 50% overcharge but at higher rates than *C*/16, e.g. *C*/8 rate for 12 h or *C*/2 rate for 3 h, gave X-ray patterns similar to Figs. 1c and d, i.e. contained largely β-NiOOH on the surface but γ-NiOOH in the interior. This observation agrees with that of Tuomi [14] and also Kuchinskii and Ershler [25] inasmuch as charging of the electrode starts closest to the main current collector and spreads outwards through the remaining electrode. Thus the interior of the sintered plate electrode, having a central main current collector, would be expected to show a greater tendency to reach a higher oxidation state (γ-NiOOH).

Although, controlled chemical oxidation processes are claimed [24, 26] to enable the production of pure β-NiOOH·xH$_2$O devoid of γ-NiOOH, it is difficult to produce pure β-NiOOH by electrochemical methods in strongly alkaline solution (7 M KOH). Briggs [27] citing the work of Aleshkevich *et al.* [28] points out from considerations of the energy to remove a proton from an OH group attached to the nickel cation that kinetic factors would tend to favour the formation of Ni(IV) rather than Ni(III).

The existence of an intermediate phase having a nickel oxidation state of ~ 2·7 during the oxidation of β-Ni(OH)$_2$ has lead to the suggestion of a compound $Ni_3O_2(OH)_4$ [2]. Whether this material is a true compound, or a phase-limit in a solid-solution system is difficult to establish because the diffraction pattern claimed for $Ni_3O_2(OH)_4$ can be accounted for by a mixture of β-Ni(OH)$_2$ and β-NiOOH. According to Bode [29], $Ni_3O_2(OH)_4$ might be considered as a transition point in the internal structural rearrangements during the chemical oxidation of β-Ni(OH)$_2$ to β-NiOOH.

Table 1 summarizes the results of the active oxygen determinations for electrodes after charging at various rates and also after discharging at the *C*/1 rate to failure at a 100 mV end point. A nickel oxidation state of 3·5 is well within the range 3·3–3·7 reported [14, 23, 24] for the γ-phase. Throughout the present work the γ-phase will be denoted simply as γ-NiOOH but the presence of Ni(IV) should not be overlooked. The observed oxidation state for the β-phase appears to be in the range 2·9–3·1 reported [14, 23, 24] for β-NiOOH but the presence of γ-phase contamination should also be noted. It is also apparent from Table 1 that appreciable quantities of higher nickel oxides remain in the electrode after discharge at the *C*/1 rate to a 100 mV end point (nickel oxidation state 2·3–2·6).

Table 2 gives the levels of K^+ ions found in electrodes in various stages of charge and discharge. The results have been corrected for the quantity of K^+ held in the pores by subtracting the value for uncharged electrodes steeped in 30% KOH. This corresponds to the volume of KOH calculated to occupy the available pore volume in the electrode (0·23 ml). It has been reported [14, 15, 24] during formation of γ-NiOOH that K^+ ions are taken into the lattice but on discharge are ejected. Bode *et al.* [24] found a Ni/K ratio of 3·0 compared with 2·5–3·1 in this investigation. In contrast it has been observed [24] that there is little if any uptake of K^+ during formation of pure β-NiOOH. The small uptake of K^+ by the mainly β-phase materials prepared in this investigation is most probably caused by contaminination with γ-NiOOH. From Table 2 it can be shown that for electrodes which contain only γ-NiOOH the K^+

Table 1. Average oxidation states of active material

Charge regime	*Average oxidation state of charged electrode*	*Average oxidation state of discharged electrodes, C/1 rate to 100 mV*
C/2 for 12 h	3·5	2·6
C/2 for 3 h	3·1	2·4
C/8 for 12 h	3·0	2·4
C/16 for 24 h	2·9	2·3

Table 2. K^+ levels for electrodes at various stages of charge and discharge

Charge regime	*Principal phase*	*K^+ levels* (mg)*		
		Charged	*Discharged C/1 to 100 mV*	*Discharged C/1 to 100 mV then C/50 to H_2 evolution*
C/2 for 12 h	γ-NiOOH	123 ± 13	60 ± 5	27 ± 2
C/2 for 3 h	β-NiOOH	43 ± 4	17 ± 1	10
C/8 for 12 h	β-NiOOH	39 ± 1	13 ± 1	8 ± 6
C/16 for 24 h	β-NiOOH	26 ± 3	12 ± 2	7 ± 1

* Blank for steeped electrode (60 ± 3 mg) subtracted.

ion to capacity ratio is ~ 0·38 mg K^+/mA h. This value applies to both fully charged and *C*/1 rate discharged states. On this basis it may be deduced for example for the β-phase material obtained by charging at the *C*/16 rate for 24 h that the electrode contains ~ 80% of a material having an oxidation state of 2·75 and ~ 20% γ-NiOOH (oxidation state 3·5). This would be consistent with the X-ray data and substantiates the view that pure β-NiOOH having a nickel oxidation state of 3 is difficult to obtain. Depending on the experimental conditions such as electrolyte concentration and temperature, oxidation of β-$Ni(OH)_2$ may stop at near $Ni^{2\cdot75+}$, the remaining charge being used in oxygen evolution. Alternatively further oxidation as in this case takes place to the γ-phase without the necessity of complete conversion to β-NiOOH. These observations are confirmed by recent equilibrium potential measurements which are to be reported [18].

3.2. *Comparison of discharge behaviour for β-NiOOH and γ-NiOOH*

Fig. 2 compares typical discharge curves for electrodes charged at the *C*/2 rate for 12 h with those subjected to the three 50% overcharge regimes. The electrode charged at the *C*/2 rate for 12 h containing predominantly γ-NiOOH shows an almost horizontal discharge plateau at ~ + 295 mV compared with the higher potential sloping plateau (+ 350 to + 300 mV) for the other electrodes containing largely β-NiOOH. Russian workers [16, 17] have also observed that the γ-phase discharges at a lower potential than the β-phase and within a narrower range of potentials. As will be shown in a further publication [18] the potential separations in the discharge curves are a consequence of the different standard potentials for the α-$Ni(OH)_2$/γ-NiOOH and β-$Ni(OH)_2$/β-NiOOH couples respectively. Both systems can be shown to exhibit horizontal, heterogeneous discharge characteristics. Conway and Gileadi [30] found for essentially β-phase starting materials that the reversible potential was constant for degrees of oxidation between ~ 10% and ~ 50%. Thus the central sloping region observed in Fig. 2 for the discharge of largely β-phase materials can be considered to arise from the discharge of mixed-phases rather than homogeneity within a single solid phase.

During on-load conditions additional concentration polarization effects will also be present. Towards the later stages of discharge, the shape of the discharge curve approaches that for the pure γ-phase. This is because the pure β-phase discharges first at a higher potential leaving behind the γ-phase impurity.

Conway and Gileadi [30] considered that the constant potential region was derived from a surface layer of constant composition superimposed on a bulk phase of varying degree of oxidation but not potential determining. Alternatively, reversible potentials for the β-$Ni(OH)_2$/β-NiOOH and α-$Ni(OH)_2$/γ-NiOOH couples could be considered as being established by a heterogeneous mechanism between certain fixed solid-solubility limits defined by the composition/free energy relationships [18]. Near to the limits of oxidation and reduction it is likely that a homogeneous process is involved but for the greater part of the operating range the potential is held constant by the equilib-

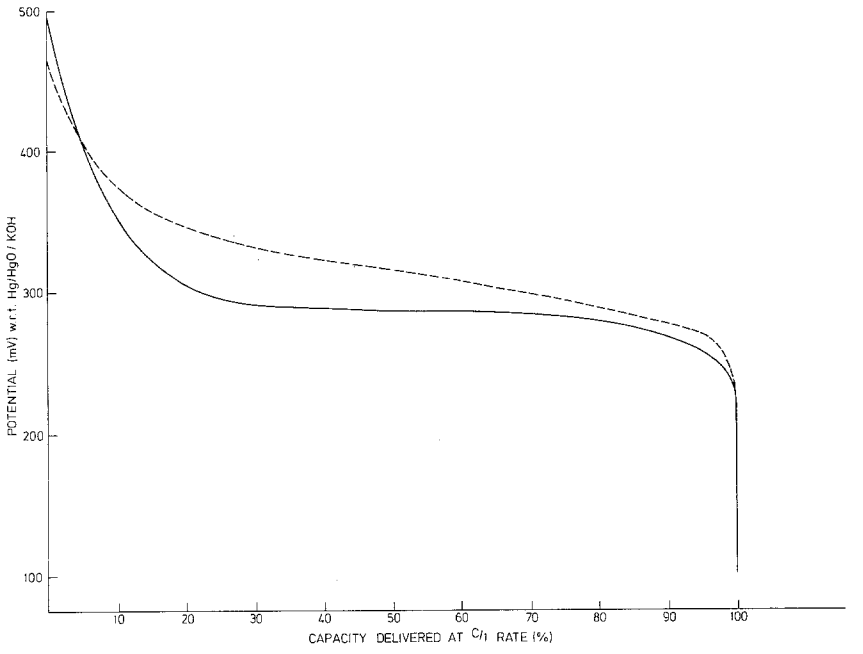

Fig. 2. Galvanostatic discharge curves ($C/1$ rate) for sintered plate electrodes charged at various rates. —— Electrodes charged at the $C/2$ rate for 12 h (mainly γ-NiOOH). - - - - - Electrodes charged at the $C/12$ rate for 24 h or $C/8$ rate for 12 h or $C/2$ rate for 3 h (mainly β-NiOOH).

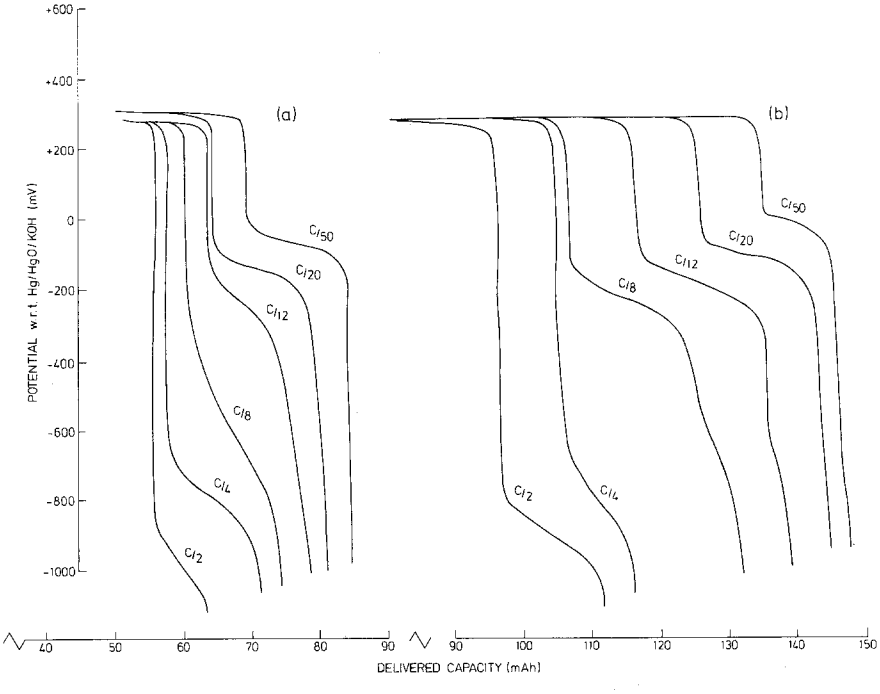

Fig. 3. Secondary potential discharge steps obtained at various discharge rates (indicated on the diagram) for: (a) Plates charged at the $C/16$ rate for 24 h (mainly β-NiOOH); (b) Plates charged at the $C/2$ rate for 12 h (mainly γ-NiOOH).

rium between pairs of mutual solid solutions containing lower and higher valent nickel species [18].

Figs. 3a and b are the later parts of the potential–time curves obtained during discharge of β- and γ-NiOOH respectively at various rates. Similar steps may be generated by lowering the discharge rate after failure at the $C/1$ rate. In this case discharge continues for a short period at ~ + 350 mV before the step appears. The potential of the lower plateau is highly dependent on discharge rate and also to some extent on the charge regime applied to the electrode. This plateau is unlikely to be due to the discharge of adsorbed molecular oxygen. The large and variable capacity involved together with the black colour of the active material after discharge at the $C/1$ rate implies the presence of large quantities of higher nickel oxides. The electrodes only resumed their original greyish-green colour after the second discharge plateau was completed and hydrogen evolution reached.

Diffraction patterns were also recorded for electrodes which had been discharged to failure at the $C/1$ rate (+ 100 mV end point). Figs. 4a and b are respectively complete and powdered electrode samples relating to discharged electrodes previously charged at the $C/2$ rate for 12 h. Fig. 4a shows lines characteristic of γ-NiOOH with only weak β-lines ($2\theta = 19°$, $35°$ and $59°$). Fig. 4b differs only in respect of the increased relative intensities of the β-lines. These lines have been assigned to β-$Ni(OH)_2$ because β-NiOOH discharges at a higher potential than γ-NiOOH and it is therefore unlikely to be produced by discharge of γ-NiOOH. Thus the residual capacity can be attributed largely to γ-NiOOH in this case.

Figs. 4c and d show patterns again for complete and powdered electrode samples but charged at the $C/16$ rate for 24 h before discharge to failure at the $C/1$ rate. Fig. 4c shows lines characteristic of only β-phase compounds. Because the intensities of the lines at $2\theta = 33°$, $37 - 38°$ are reduced relative to the line at $2\theta = 19°$ it seems likely that the pattern arises from a mixture of β-$Ni(OH)_2$ and β-NiOOH. Nevertheless, Fig. 4d shows weak lines at $2\theta = 12{\cdot}6°$ and $25{\cdot}4°$ indicative of some γ-NiOOH. From considerations of the K^+ ion contents, for electrodes charged at the $C/16$ rate for 24 h and discharged at the $C/1$ rate, it can be estimated that the γ-NiOOH probably only contributes about 32 mA h to the total residual capacity of 79 mA h. These results imply that β-NiOOH can contribute to the residual capacity as well as γ-NiOOH.

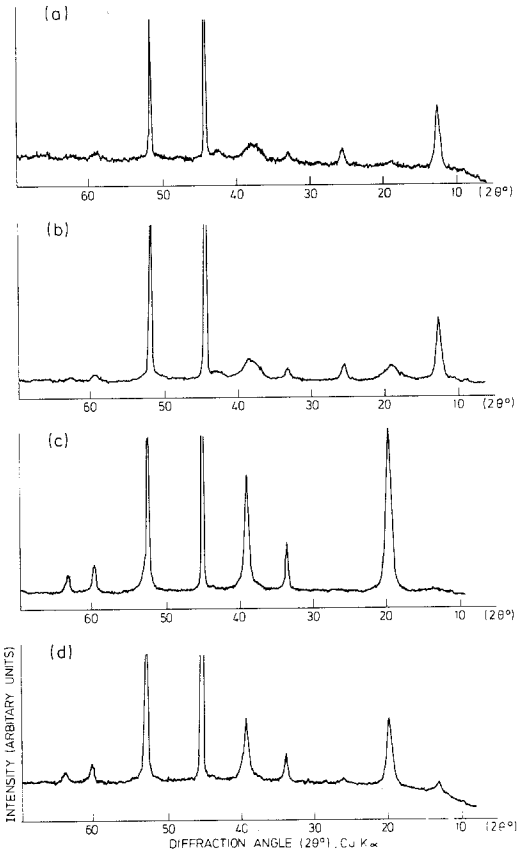

Fig. 4. X-ray diffraction patterns for γ-NiOOH and β-NiOOH electrodes discharged at the $C/1$ rate to + 100 mV w.r.t. Hg/HgO/KOH: (a) Plate initially charged at $C/2$ rate for 12 h, pattern obtained from the electrode surface; (b) As (a) but pattern obtained from a powdered sample; (c) Plate initially charged at $C/16$ rate for 24 h, pattern obtained from the electrode surface; (d) As (c) but pattern obtained from a powdered sample.

In order to determine whether a temporary diffusion restriction in the solid state was responsible for the low potential plateaux of Figs. 3a and b, electrodes after being discharged to a range of points on the lower plateaux were placed on open circuit for varying lengths of time before re-application of the $C/50$ rate discharge current. The potentials of electrodes placed on open circuit rose rapidly to between + 300 mV and + 350 mV, i.e. to the open circuit potential of a partially discharged electrode (cf. Labat [10]). When discharge was restarted after open circuit stand periods of

up to 24 h the potential fell back rapidly to that of the lower plateau with no measureable charge delivered at the potential of the upper plateau. Open-circuit periods in excess of 24 h caused a drastic fall in the charge delivered along the secondary plateau before hydrogen evolution After 107 h virtually no charge could be extracted from the electrodes. Because the electrodes were black in colour it is unlikely that the self-discharge was so great as to cause total loss of capacity. This suggests that during standing an ageing process takes place. The secondary plateau is unlikely therefore to be caused by a diffusion limitation.

Slow cathodic voltametric sweeps (5·5 mV min^{-1}) were also performed on electrodes after discharge to failure at the *C*/1 rate. The results are presented in Fig. 5a and c for N_2 saturated electrolyte where it can be seen that broad humps are obtained extending from 0 to − 500 mV irrespective of the initial charging conditions (i.e *C*/2 for 12 h or *C*/16 for 24 h). The peaks near + 300 mV are due to the discharge of small amounts of normal charged active material remaining after the high rate galvanostatic discharge. Figs. 5b and d are similar curves obtained with O_2 saturated electrolyte. The most significant change appears to be the increased background current over the whole potential range but in particular near − 800 mV. According to Shumilova and Bagotzky [31] reduction of O_2 to H_2O_2 is inhibited by $Ni(OH)_2$ films on Ni. Thus O_2 evolution would be expected to occur more readily at potentials approaching hydrogen evolution where the thin hydroxide films on the sinter are removed (~ − 890 mV). It is concluded that although some O_2 reduction appears to be possible in the potential range 0 to − 500 mV the broad humps do not originate primarily from this process. Whether or not O_2 increases the sizes of the humps is difficult to ascertain because of the variability between the electrode samples. It is clear that the broad humps in the region 0 to − 500 mV correlate with the low potential plateaux observed during galvanostatic discharge.

3.3. *Relationship between the charged active material and the residual capacity*

Fig. 6a–d summarizes the results of galvanostatic discharge and active oxygen measurements on electrodes subjected to different charge regimes. As expected the highest charge acceptance was achieved for electrodes charged at the *C*/2 rate for 12 h. For the three 50% overcharge regimes the charge acceptance decreased slightly as the charge rate was lowered [1]. Similarly the useful capacity delivered at the *C*/1 rate to failure (+ 100 mV) decreased as the charge acceptance decreased. The capacity remaining after failure for electrodes subjected to the 50% overcharge regimes was almost constant (about 35% of the total charge accepted) but was slightly higher (40%) for electrodes charged at the *C*/2 rate for 12 h. Secondary discharge at the *C*/50 rate further reduced the residual capacity. The charge remaining varied from sample to sample but on average was about 10% of that for a fully charged electrode.

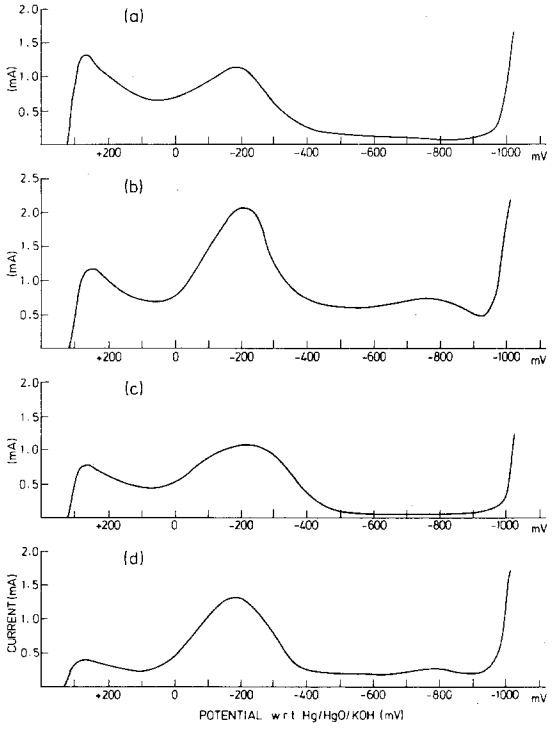

Fig. 5. Cyclic voltammograms obtained for electrodes after galvanostatic discharge at *C*/1 rate to + 100 mV w.r.t. Hg/HgO/KOH. Sweep rate, 5·5 mV min^{-1}; (a) $Ni(OH)_2$ electrode initially charged at the *C*/2 rate for 12 h; voltammogram obtained in N_2 saturated electrolyte; (b) As (a) but voltammogram obtained in O_2 saturated electrolyte; (c) $Ni(OH)_2$ electrode initially charged at the *C*/16 rate for 24 h, voltammogram obtained in N_2 saturated electrolyte; (d) As (c) but voltammogram obtained in O_2 saturated electrolyte.

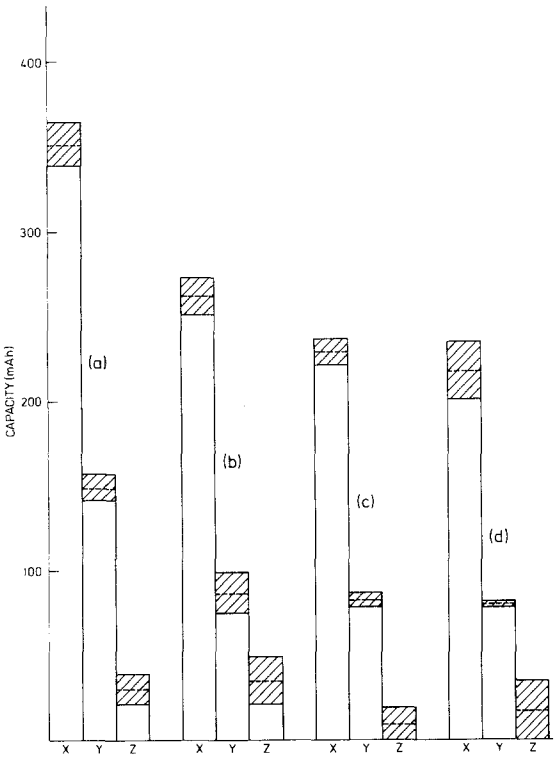

Fig. 6. Diagram comparing the relative levels of capacity for electrodes subjected to various charge regimes, (a) $C/2$ rate for 12 h; (b) $C/2$ rate for 3 h; (c) $C/8$ rate for 12 h and (d) $C/16$ rate for 24 h, where: X denotes the total capacity accepted; Y is the capacity remaining after discharge at the $C/1$ rate to + 100 mV w.r.t. Hg/HgO/KOH and Z is the capacity remaining after discharge at $C/50$ to H_2 evolution (— 1000 mV w.r.t. Hg/HgO/KOH). - - - - - indicates mean value determined whilst shaded-areas correspond to the range obtained for seven determinations in each case.

The high capacity (202 mA h) delivered during discharge at the $C/1$ rate for electrodes containing only γ-NiOOH (Fig. 6a) is in disagreement with Tuomi's claim [14] that γ-NiOOH is not readily dischargeable at high rates. Although slightly greater residual capacities were found for these electrodes this is more than offset by the greater charge accepted during γ-phase formation. By comparison electrodes containing essentially β-NiOOH gave useful capacities in the range 175–139 mA h, (Figs. 6b–d). Our observations are in agreement with those of the Russian workers [16, 17].

3.4. *Cause of residual capacity*

X-ray diffraction studies and capacity measurements have shown that the residual capacity cannot be specifically associated with the charged active material being either β- or γ-NiOOH. Similarly adsorbed oxygen is unlikely to be a major contributor.

The classical explanation [2–6] for the lower potential plateau is the discharge of a less active intermediate phase such as $Ni_3O_2(OH)_4$ or $4\,Ni(OH)_2 \cdot NiOOH$. It has been shown after allowing for contamination of the β-phase by a small quantity of the γ-phase that the pure β-phase system operated over the nickel oxidation range from ~ 2·75 to 2·25. As $Ni_3O_2(OH)_4$ corresponds to an oxidation state of 2·67 the remaining active material can hardly be this compound. However, a material nearer in composition to $4\,Ni(OH)_2 \cdot NiOOH$ discussed by Glemser and Einerhand [2] could be responsible. Because potentials in the nickel oxyhydroxide system corresponding to the secondary almost horizontal discharge steps are only observed under dynamic conditions it is unlikely that the secondary discharge steps relate to equilibrium processes. The marked dependence of the secondary plateau potential on current (Fig. 3) is further evidence against such an equilibrium process. It is considered more likely that the low potential plateau and the broad peak centred near — 200 mV during the voltammetric sweeps represents a non-equilibrium process involving removal of essential defects in returning nickel to the divalent state. Pure α- and β-$Ni(OH)_2$ are electronic insulators or low conductivity p-type semiconductors [14]. The presence of Ni^{3+} or Ni^{4+} defects are necessary to confer electronic conductivity (n-type semiconductivity [32]). In the secondary plateau region because of the relative ease of passing current in the charge direction compared to the difficulty in the discharge direction, this behaviour is analogous to that of a forward and reverse biased semiconductor diode. Thus it could be proposed that the secondary discharge step arises from the behaviour of a mixed, pn-semiconducting material under reverse bias conditions. This model will be considered in detail in the later paper [18].

Residual capacity can be related in the first instance to the minimum level of Ni^{3+} or Ni^{4+} defects in a single homogeneous phase which are required to render the $Ni(OH)_2$ sufficiently electronically conducting at a particular discharge

current density. It is also possible that this composition is near to that for the least oxidized co-existing phase component. At high rates of discharge premature isolation can be induced such that a relatively thin divalent zone can isolate an inordinately large amount of otherwise usable active material. Several workers [12, 13, 25, 33, 34] have provided visual evidence for this type of behaviour. The extent to which isolation of active material occurs depends on the number and proximity of the current collectors which is in turn largely governed by the type of electrode fabrication. Loosening of active material, with subsequent loss of electrical contact can also be caused by gas evolution or by expansion and contraction of the active material on charge and discharge.

Residual capacity can be considered to arise therefore from two sources; the first is a consequence of the thermodynamic/electronic conductivity requirements whilst the second is an artefact related to the electrode fabrication. It is this latter factor which is responsible for the high variability in the levels of residual capacity observed in practice. As a consequence it is difficult to establish with certainty the oxidation state corresponding to the least oxidized co-existing phase component. Clearly the values obtained for the oxidation states of nickel after discharge of β- or γ-phase (Table 1) suggest that a significant proportion of the upper oxidation state remains isolated in the active material.

Acknowledgements

The authors wish to thank the Directors of the Berec Group Ltd for permission to publish this work.

References

[1] P. Kelson, A. D. Sperrin and F. L. Tye, 'Power Sources', Vol. 4, edited by D. H. Collins, Oriel Press (1973) p. 201.
[2] O. Glemser and J. Einerhand, *Z. Elektrochem.* **54** (1950) 302.
[3] S. E. S. El Wakkard and E. S. Emara, *J. Chem. Soc.* 4 (1953) 3504.
[4] J. Besson, *Ann. Chim.* **2** (1947) 527.
[5] A. P. Rollet, *ibid* **13** (1930) 217.
[6] F. Foerster, 'Elektrochemie Wassrigen Losungen' edited by J. A. Barth, 3rd ed., Leipsig (1922) p. 265.
[7] J. Zedner, *Z. Elektrochem.* **12** (1906) 463.
[8] *Idem*, *ibid* **13** (1907) 752.
[9] H. Bode, K. Dehmelt and H. Von Dohren, *Proceedings 2nd International Symposium on Batteries*, Bournemouth (1960) paper 6/1.
[10] J. Labat, *Ann. Chim.* 9 (1964) 399.
[11] S. U. Falk, *J. Electrochem. Soc.* **107** (1960) 662.
[12] G. W. D. Briggs, E. Jones and W. F. K. Wynne-Jones, *Trans. Faraday Soc.* **51** (1955) 1433.
[13] *Idem*, *ibid* **52** (1956) 1260, 1272.
[14] D. Tuomi, *J. Electrochem. Soc.* **112** (1965) 1.
[15] J. P. Harivel, B. Morignat, J. Labat and J. F. Laurent, 'Power Sources' edited by D. H. Collins (1966) p. 239.
[16] E. A. Keminskaya, N. Yu. Uflyand and S. A. Rozentsveig, *Sbornik. Rab. Khim. Istochnikam Toka* 4 (1969) 13.
[17] N. Yu. Uflyand, A. M. Novakovskii and S. A. Rozentsveig, *Elektrokhimiya* 3 (1967) 537.
[18] R. Barnard, C. F. Randell and F. L. Tye, *J. Appl. Electrochem.* **10** (1980) 109.
[19] H. H. Kroger and A. J. Catotti, *Proceedings 24th International Power Sources Symposium*, (1970) p. 4.
[20] H. P. Klug and L. E. Alexander, 'X-Ray Diffraction Procedures' J. Wiley and Sons (1954) p. 491.
[21] F. J. Micale, M. Topic, C. L. Cronan, H. Leidheiser, A. C. Zettlemayer and S. Popovic, *J. Col. Interface Sci.* 55 (1976) 540.
[22] D. Louer, D. Weigl and J. I. Langford, *J. Appl. Cryst.* 5 (1972) 353.
[23] O. Glemser and J. Einerhand, *Z. Anorg. Chem.* **261** (1950) 26, 43.
[24] H. Bode, K. Dehmelt and J. Witte, *Z. Anorg. Allg. Chem.* **366** (1969) 1.
[25] B. V. Ershler and E. M. Kuchinskii, *Zh. Fiz Chem.* **20** (1946) 539.
[26] H. Bode, K. Dehmelt and J. Witte, *Electrochim. Acta* **11** (1966) 1079.
[27] G. W. D. Briggs, *Chem. Soc. Specialist Periodical Reports, Electrochemistry* **4** (1974) 37.
[28] S. A. Aleshkevich, E. J. Golovchenko, V. P. Morozov and L. N. Sagoyan, *Soviet Electrochem.* 4 (1968) 530, 1117.
[29] H. Bode, *Angew. Chem.* 73 (1961) 553.
[30] B. E. Conway and E. Gileadi, *Canad. J. Chem.* 40 (1962) 1933.
[31] N. A. Shumilova and V. S. Bagotzky, *Electrochim. Acta* **13** (1968) 285.
[32] A. A. Yakovleva and Yu. N. Chernykh, *Electrokhimiya* 6 (1970) 1671.
[33] G. W. D. Briggs and W. F. K. Wynne-Jones, *Electrochim. Acta* 7 (1962) 241.
[34] G. W. D. Briggs and M. Fleischmann, *Trans. Faraday Soc.* 67 (1971) 2397.